Numerical Simulation of Natural Convection in a Chamfered Square Cavity with Fe_3O_4-Water Nanofluid and Magnetic Excitation

Rached Nciri
Department of Mechanical Engineering, Higher Institute of Technological Studies of Gafsa, General Directorate of Technological Studies, Rades Medina 2098, Tunisia
rachednciri@yahoo.fr

Ala Eldin A. Awouda
Department of Mechanical Engineering, College of Engineering, University of Bisha, Bisha, 61922, P.O. Box 001, Saudi Arabia
aadam@ub.edu.sa

Amir Abubaker Musa
Department of Mechanical Engineering, College of Engineering, University of Bisha, Bisha, 61922, P.O. Box 001, Saudi Arabia
aamusaa@ub.edu.sa (corresponding author)

Hamod Ghorm Alshomrani
Saudi Electricity Company, Saudi Arabia
alrahal2000@hotmail.com

Faouzi Nasri
Department of Mechanical Engineering, College of Engineering, University of Bisha, Bisha, 61922, P.O. Box 001, Saudi Arabia
nasrifaouzi@yahoo.fr

Received: 29 November 2024 | Revised: 15 December 2024 and 24 December 2024 | Accepted: 1 January 2025

 DOI: https://doi.org/10.48084/etasr.9775

ABSTRACT

This study delves into the numerical exploration of the MagnetoHydroDynamic (MHD) characteristics of an Fe_3O_4-Water nanofluid contained within a chamfered square enclosure under the influence of an external magnetic field. The enclosure, characterized by distinct hot and cold imposed temperatures on its side walls, features both straight and chamfered sections. The orientation of magnetic field lines was manipulated by varying the angular placement of the magnetic source. The computational framework for nanofluid dynamics is mathematically formalized through a dimensionless formulation of the Navier-Stokes equations derived from their dimensional counterparts. A comprehensive numerical analysis was conducted employing the Finite Element (FE) method, a. The interaction between the Hartmann number and the angular placement of the magnetic source was analyzed, with a specific focus on nanofluid isotherms, temperature profiles, and velocity magnitude distributions. The results were thoroughly investigated and extensively discussed.

Keywords-MHD; nanofluid; chamfered squared cavity; Navier-Stokes model; isotherms; temperature distribution; velocity magnitude distribution; Hartmann number

I. INTRODUCTION

Nanofluids [1-4] consist of a base fluid and dissolved nanoparticles in suspension. The base fluid can be water, oil, ethylene glycol or others while nanoparticles can be metals, oxides, carbon-based, or others. The base fluids, presenting the medium for dispersing nanoparticles, ensure stability and good heat transfer capabilities whereas nanorpaticles significantly

boost the thermal conductivity of the base fluid. Their incredibly small size, usually less than 100 nm, permits to improve the capacity of the fluid to transfer heat, enhancing its overall efficiency in heat dissipation. Some interesting research works of the past three years can be pointed out from the literature. Authors in [5] investigated the hydrothermal behavior of nanofluid flow within a hexagonal cavity featuring an inner circular cylinder equipped with various rectangular fins. The upper and bottom cavity walls were heated while the other walls re-main cold. Numerical results in terms of streamline, isotherm, and Nusselt number profile plots were generated to evaluate the impact of Rayleigh number, Hartmann number, and nanoparticle volume fraction on the flow, considering different fin lengths. The results indicate that increasing the Rayleigh number amplifies convection, velocity, and heat transfer. Conversely, higher Hartmann numbers and concentrations of nanoparticles lead to reduced velocity components. Authors in [6] studied the natural convective flow and heat transfer within an enclosure containing a hybrid nanofluid, with multiple heat sources positioned at the enclosure's bottom wall, in the presence of a magnetic field oriented at an angle to the horizontal axis. The main results highlight significant alterations in the flow pattern due to variations in the magnetic field parameter, angle of the magnetic field, number, and size of heat sources, and the Rayleigh number. Authors in [7] carried out a numerical investigation examining the impact of an anti-rotational magnetic field in contrast to the rotation of an Al_2O_3-water nanofluid in an inclined triangular cavity with bottom heating and top cooling, experiencing buoyancy-driven flow. The rotational influences were investigated through steady simulations at various cavity inclinations. The heat source was positioned at the right-angled corner, partially spanning the adjacent sides of equal length. A cooling source of equivalent size was symmetrically placed on the hypotenuse around the vertical axis. Parameters under study encompass the Rayleigh number, concentration of Al_2O_3-water nanofluid, Hartmann number, cavity orientation, and magnetic field orientation. Authors in [8] conducted a numerical study of magneto-convection heat transfer using an Ag-based nanofluid (comprising silver nanoparticles dispersed in a fluid) within a square enclosure housing a thin central heater and a lower section of the heated wall. The investigation primarily examined the impact of the magnetic field strength, orientation and length of the central heater, length of the lower heated wall section, Rayleigh number, and volume fraction of the Ag nanoparticles on the average Nusselt number along the vertical, cooled sidewalls of the enclosure. The analysis revealed that heightened heat transfer performance aligns with increased lengths of the central heater and the lower heated wall section. Moreover, an increase in the average Nusselt number was observed with a vertically oriented central heater. Irrespective of the heater's orientation, heat transfer efficiency diminishes as the magnetic field strength increases. With an escalation in the Ag nanoparticle volume fraction, the average Nusselt number increases, especially with higher Rayleigh number values. Notably, at high Rayleigh numbers of 106 and 107, enhanced heat transfer performance was documented with increasing nanoparticle volume fractions: 0.00, 0.03, 0.06 and 0.09. Authors in [9] conducted simulations focused on free convective heat transfer and entropy generation within a closed enclosure. Constant volumetric radiation was generated within the cavity, which is positioned at a 45° angle relative to the horizon. Increasing the Hartmann number resulted in reduced Nusselt number on both heated walls and a decrease in fluid flow within the enclosure. Authors in [10] studied the flow and thermal behavior of MHD Casson nanofluid within a square enclosure featuring a non-uniform heat source on the bottom wall. The analysis showcased the influence of governing parameters on local Nusselt number, streamlines, and isotherms. The visualization revealed the presence of two counter-rotating vortices in the streamlines, stemming from buoyancy effects caused by temperature variations along the enclosure's side with non-uniform temperature distribution. An increase in the Rayleigh number induces a marked temperature rise in the enclosure's center, while the thermal distribution became more pronounced near the enclosure walls. Authors in [11] investigated the natural convective flow dynamics and heat transfer influenced by a magnetic field within a concentric circular annulus. This annulus was situated between a heat-generating inner cylinder and an externally cold cylinder filled with a CNTs-water-based nanofluid. The natural flow rose from the temperature gradient between the heat-generating inner cylinder and the outer cold cylinder.

This study presents a significant novelty in MHD research by investigating Fe_3O_4-water nanofluid behavior in a chamfered square enclosure under a variable angular magnetic field, a rarely studied configuration. Unlike prior works focused on regular geometries or static fields, it uniquely examines the combined effects of chamfered design and dynamic magnetic orientation. The findings on Hartmann number and magnetic source angle interactions provide novel insights for controlling nanofluid flow and heat transfer.

II. PROBLEM STATEMENT

A Fe_3O_4 nanofluid [12-14] with the thermophysical properties summarized in Table I is considered. As shown in Figure 1, the considered nanofluid is filled in a chamfered square cavity with an external magnetic source. Hot and cold temperature are respectively imposed at the right and left walls while other walls are considered adiabatic.

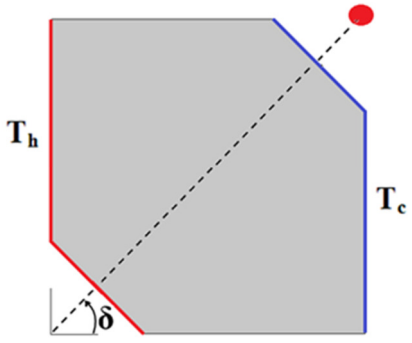

Fig. 1. Problem description.

TABLE I. THERMOPHYSICAL PROPERTIES OF THE Fe_3O_4 NANOFLUID

Thermophysical properties	Magnetic particles (Fe_3O_4)	Fluid (Water)
Density ρ	5180 kg/m^3	997.1 kg/m^3
Thermal conductivity k	9.7 W/mK	0.613 W/mK
Specific heat capacity C_p	670 J/kgK	4179 J/kgK

III. MATHEMATICAL MODEL

A. Model Assumptions

The considered nanofluid is supposed to be Newtonian, incompressible (since the base fluid is water with a volume fraction) with a density variation under the Boussinesq approximation [15-18]. The nanofluid flow is supposed 2D, steady, and laminar. The induced displacement currents, magnetic field, and Joule heating are considered negligible. Radiation and energy dissipations are also supposed negligible [19].

B. Dimensionless Model

1) Dimensionless Quantities

To allow scaling between different system dimensions and conditions, it is highly useful to make the model dimensionless. The dimensionless quantities, constituting the dimensionless model, are summarized in Table II.

TABLE II. DIMENSIONLESS QUANTITIES

$X=\frac{x}{L}$	$Y=\frac{y}{L}$	$U=\frac{uL}{\alpha_{nf}}$	$P=\frac{pL^2}{\rho_{nf}\alpha_{nf}^2}$
$\theta=\frac{T-T_c}{T_h-T_c}$	$V=\frac{vL}{\alpha_{nf}}$	$\Pr^*=\frac{\upsilon_{nf}}{\alpha_{nf}}$	$Ra^*=\frac{g\beta(T-T_c)L^3}{\upsilon_{nf}\alpha_{nf}}$
$Ha^*=LB_0\sqrt{\frac{\sigma_{nf}}{\mu_{nf}}}$		$\overline{H}_x=\frac{I}{2\pi}\frac{1}{(x-a)^2+(y-b)^2}(y-b)$	
$\overline{H}_y=\frac{I}{2\pi}\frac{1}{(x-a)^2+(y-b)^2}(x-a)$		$H_0=\sqrt{\overline{H}_x{}^2+\overline{H}_y{}^2}=\frac{I}{2\pi}\frac{1}{\sqrt{(x-a)^2+(y-b)^2}}$	
$H=\frac{\overline{H}}{H_0}$		$Ec^*=\frac{\mu_{nf}\alpha_{nf}}{(\rho C_p)_{nf}L^2\Delta T}$	

2) Dimensionless Mass Conservation Equation

$$\frac{\partial U}{\partial X}+\frac{\partial V}{\partial Y}=0 \quad (1)$$

3) Dimensionless x-Momentum Equation

$$U\frac{\partial U}{\partial X}+V\frac{\partial U}{\partial Y}=-\frac{\partial P}{\partial X}+\Pr^*\left(\frac{\partial^2 U}{\partial X^2}+\frac{\partial^2 U}{\partial Y^2}\right)+F_x \quad (2)$$

with:

$$F_x=-Ha^{*2}\Pr^* H_y^2 U+Ha^{*2}\Pr^* H_x H_y V \quad (3)$$

4) Dimensionless y-Momentum Equation

$$U\frac{\partial V}{\partial X}+V\frac{\partial V}{\partial Y}=-\frac{\partial P}{\partial Y}+\Pr^*\left(\frac{\partial^2 V}{\partial X^2}+\frac{\partial^2 V}{\partial Y^2}\right)+F_y \quad (4)$$

with:

$$F_y=Ra^*\Pr^*\theta-Ha^{*2}\Pr^* H_x^2 V+Ha^{*2}\Pr^* H_x H_y U \quad (5)$$

5) Dimensionless Energy Conservation Equation

$$U\frac{\partial \theta}{\partial X}+V\frac{\partial \theta}{\partial Y}=\left(\frac{\partial^2 \theta}{\partial X^2}+\frac{\partial^2 \theta}{\partial Y^2}\right)+\Theta_T \quad (6)$$

with:

$$\Theta_T=Ec^*Ha^{*2}(H_x V-H_y U)^2+Ec^*\left\{2\left(\frac{\partial U}{\partial X}\right)^2+2\left(\frac{\partial V}{\partial Y}\right)^2+\left(\frac{\partial U}{\partial X}+\frac{\partial V}{\partial Y}\right)^2\right\} \quad (7)$$

IV. RESULTS AND DISCUSSION

Figure 2 shows the combined impact of Hartmann number and the angular position of the magnetic source on the nanofluid isotherms. The results highlight the interplay between heat transfer at the walls and the magnetic field on these isotherms. It is noteworthy that near the hot and cold walls, the isotherms tend to align almost parallel to the walls, whereas near the adiabatic walls, they tend to align almost perpendicular to them. This behavior is attributed to the heat transfer processes being predominantly governed by conduction near the hot and cold walls, where heat moves from the hot wall to the adjacent nanofluid, raising its temperature. Similarly, heat is conducted from the nanofluid to the cold walls, causing the nanofluid to cool. In the vicinity of adiabatic walls, where heat transfer is restricted, the nanofluid temperature remains relatively constant, resulting in isotherms that are nearly perpendicular to the walls in this region. Away from the walls, isotherms tend to be almost parallel to the paths of magnetic field lines depending on angular locations of the magnetic source (horizontal, vertical, or intermediate). This is explained by the fact that the influence of the magnetic field becomes leading in the central region (away from the hot and cold walls). The magnetic forces impact the fluid dynamics (motion), facilitating the transfer of heat along the paths defined by the magnetic field. Results also show that as the Hartmann number increases, the alignment of the isotherms with the magnetic field paths is enhanced. The temperature gradient across the nanofluid becomes more uniform along the magnetic field paths. The heat transfer along the perpendicular direction to the magnetic field path is highly reduced, due to the enhancement of Lorentz force, as the Hartman number increases, which weakens the motion of the nanofluid. Thus, the convection is delayed and the conduction becomes more significant. It should be noted that the effect of Hartmann number is more pronounced for positive angular locations since, in this case, the magnetic source is closer to the nanofluid than when a negative angular location is considered. The closer the magnetic source is to the nanofluid, the stronger the magnetic field becomes, resulting in a more pronounced alignment of the isotherms with the magnetic field lines.

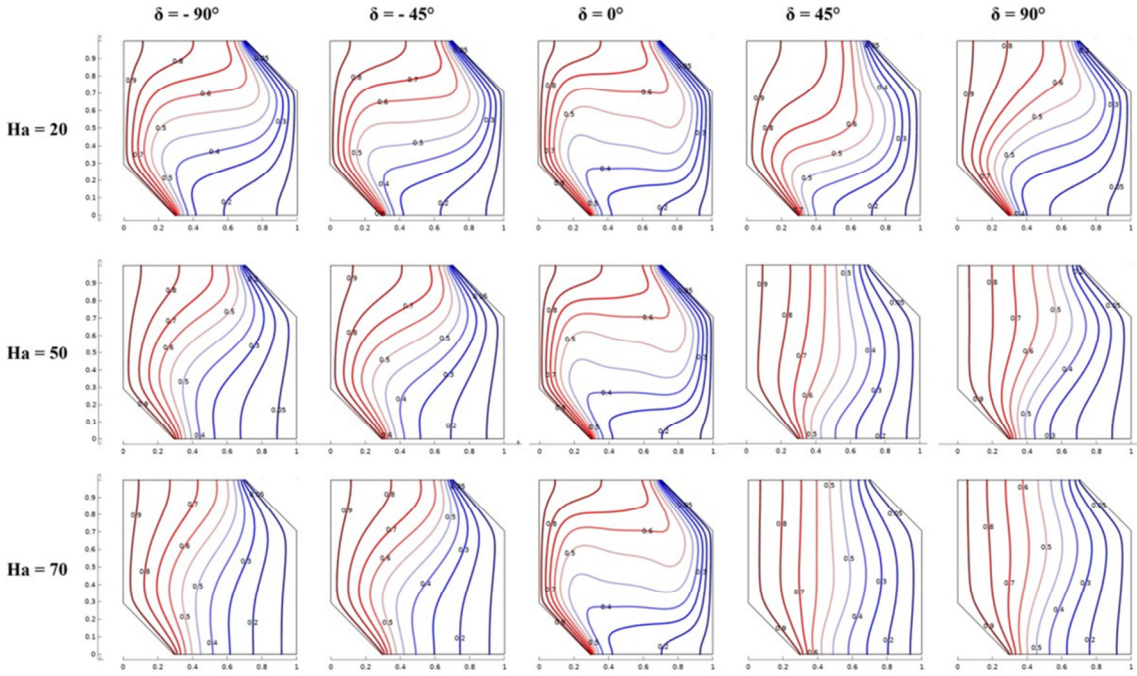

Fig. 2. Combined effect of Hartmann number and magnetic source angular location on isotherms.

Figure 3 shows the combined effect of Hartmann number and magnetic source angular location on the nanofluid temperature distribution. Results show the influence of the interaction between heat transfer at the walls and the magnetic field on temperature distribution. As the Hartmann number increases, the Lorentz forces become more significant and weaken the nanofluid motion. Therefore, convection is reduced in favor of conduction and the temperature homogeneity of the nanofluid away from the walls is deteriorated. It is important to notice that for the particular case of a horizontal magnetic source location ($\delta = 0°$), the temperature homogeneity is enhanced when the Hartmann number increases. This is explained by the fact that, in this case, the magnetic field is applied parallel to the nanofluid's flow direction (from the left hot walls to the right cold walls). In such cases, the magnetic field promotes fluid mixing which enhances the heat transfer trough convection. For angular location $\delta = 45°$ and especially $\delta = 90°$, the magnetic field is not parallel to the nanofluid flow and will restrain the motion of the charged particles in the fluid, which can lead to a significant reduction of convection in favor of conduction. As the angular location of the magnetic source varies, the heat transfer front, perpendicularly to which the temperature exhibits higher variation, is reoriented to be aligned with the magnetic field paths. The temperature homogeneity, especially away from the walls, is slightly enhanced for negative angular locations of the magnetic source due to the decrease in the magnetic field strength when the magnetic source is positioned at negative angular locations, resulting in a greater distance from the nanofluid, as opposed to positive angular locations. Thus, the nanofluid motion is improved and the convection is enhanced at the expense of conduction. Figure 4 shows the combined effect of Hartmann number and magnetic source angular location on nanofluid velocity magnitude distribution. Results show the influence of the interaction between heat transfer at the walls and the magnetic field on the velocity magnitude distribution. It is worth noting that the velocity magnitude tends to be greater within a transition region confined between the areas near the walls and the central region of the nanofluid cavity as a result of the combined effects of the magnetic field and boundary conditions. Near the walls, the non-slip condition has the dominant effect in the nanofluid. The velocity magnitude of the nanofluid is typically 0 in this region. Thus, the nanofluid near the walls is nearly stationary. In the central region, the magnetic field has a dominant effect on the nanofluid. The magnetic forces, in this region, will reduce until the velocity magnitude becomes 0. In the considered transition zone, the nanofluid escapes the dominant effects of both non-slip condition and magnetic forces. Thus, the velocity magnitude reaches the higher values in this transition region. As the Hartmann number increases, the global velocity magnitude is reduced due to the increase of the magnetic forces acting on the nanofluid for all magnetic source angular locations except $\delta = 0°$ where the velocity magnitude is not affected. This exception is explained by the fact that, for a horizontal magnetic source ($\delta = 0°$), the magnetic field and the nanofluid flow direction are parallel. The Lorentz forces, generated by the magnetic field, will act directly along the flow direction of the nanofluid (from the hot to the cold wall) since the Lorentz forces are expressed as $F_{Lorentz} = q \bullet \left(\vec{V} \times \vec{B}\right)$, where $\vec{V}$ is the velocity vector of the nanofluid and $\vec{B}$ is the magnetic field vector. When $\vec{B}$ is parallel to $\vec{V}$, i.e. when $\delta = 0°$, the cross product $\vec{V} \times \vec{B}$ is zero. Thus, the effect of Lorentz forces along the flow direction of the nanofluid is neglected and the global velocity magnitude is not altered.

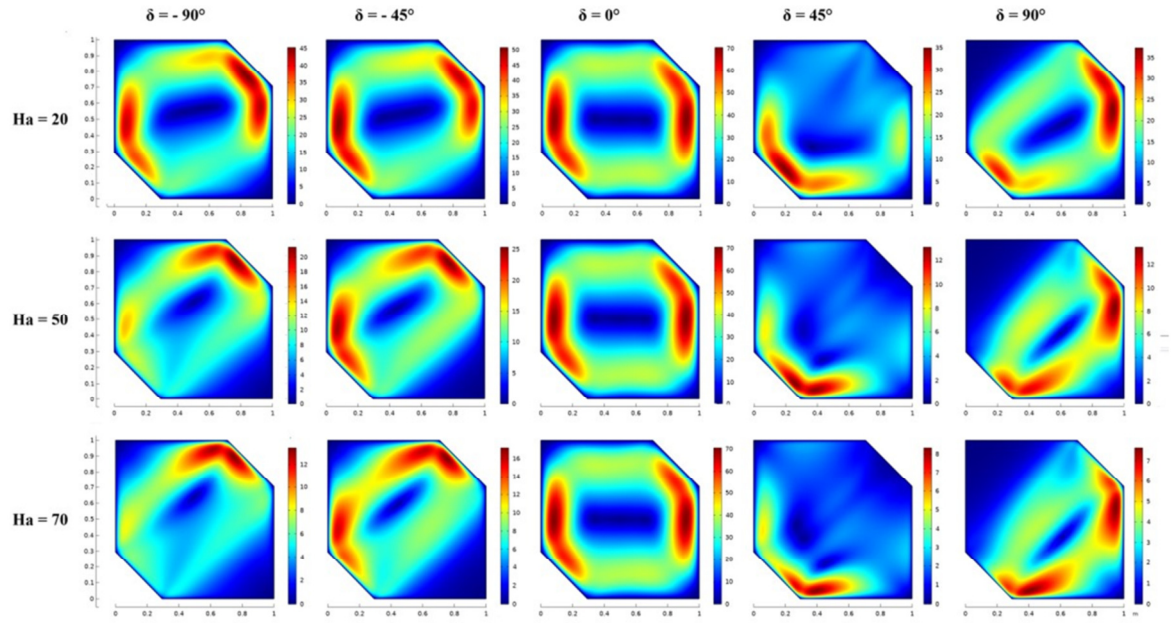

Fig. 3. Combined effect of Hartmann number and magnetic source angular location on temperature distribution.

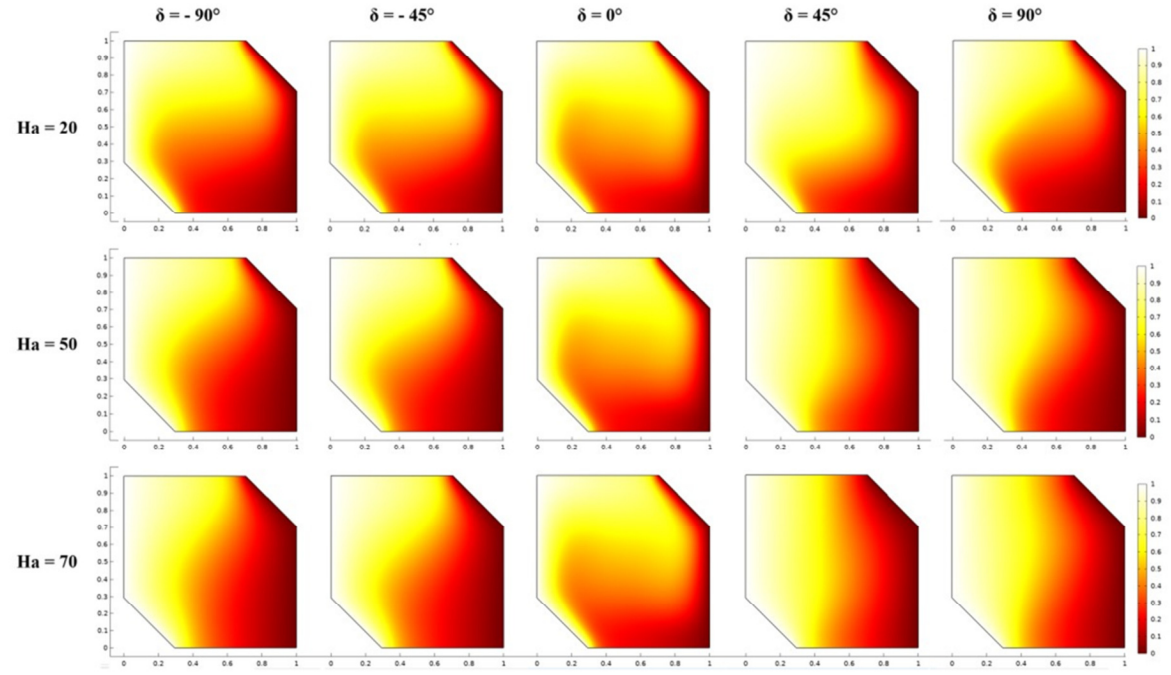

Fig. 4. Combined effect of Hartmann number and magnetic source angular location on velocity magnitude distribution.

V. CONCLUSION

In this paper, the interplay between the Hartmann number and magnetic source angular location on the MHD nanofluid behavior, in terms of isotherms, temperature distribution, and velocity magnitude distribution, was numerically investigated within a chamfered enclosure. The main findings of this research work are:

- As the Hartmann number rises, there is an improvement in the alignment between the isotherms and the paths of the magnetic field. The Hartmann number effect on the isotherms is more pronounced for positive angular positions of the magnetic source (closer magnetic source), except for an horizontal magnetic source where the Hartmann number has no effect.

- As the Hartmann number increases, the temperature homogeneity is deteriorated, except for the horizontal magnetic source where the Hartmann number enhanced the temperature homogeneity. The temperature homogeneity is slightly enhanced for negative angular positions of the magnetic source (farther magnetic source).
- As the Hartmann number increases, the velocity magnitude is deteriorating for all magnetic source angular locations except for a horizontal magnetic source where the Hartmann number has no effect.

NOMENCLATURE

B	: Magnetic induction field [T]
C_p	: Specific heat capacity [$Jkg^{-1}K^{-1}$]
g	: Gravitational acceleration [ms^{-2}]
H	: Magnetic field strength [Am^{-1}]
Ha	: Hartman number [-]
k	: Thermal conductivity [$Wm^{-1}K^{-1}$]
L	: Characteristic length [m]
p	: Pressure [Pa]
T	: Temperature [K]
u	:x-component of velocity [ms^{-1}]
v	:y-component of velocity [ms^{-1}]
α	: Thermal diffusivity [m^2s^{-1}]
β	: Coefficient of thermal expansion [K^{-1}]
ϕ	: Solid volume fraction [-]
μ	: Dynamic viscosity [Pas]
θ	: Dimensionless temperature [-]
ρ	: Density [kgm^{-3}]
σ	: Electrical conductivity [Sm^{-1}]
υ	: Kinematic viscosity [m^2s^{-1}]
c	: cold [-]
f	: Fluid [-]
h	: Hot [-]
nf	: Nanofluid [-]
p	: Particle [-]

ACKNOWLEDGMENT

The authors are thankful to the Deanship of Graduate Studies and Scientific Research at University of Bisha for supporting this work through the Fast-Track Research Support Program.

REFERENCES

[1] M. Hatami and D. Jing, "Introduction to nanofluids," in *Nanofluids: mathematical, numerical, and experimental analysis*, Cambridge, MA, USA: Academic Press, 2020, pp. 1–50.

[2] M. Hatami and D. Jing, "Mathematical analysis of nanofluids," in *Nanofluids: mathematical, numerical, and experimental analysis*, Cambridge, MA, USA: Academic Press, 2020, pp. 51–111.

[3] M. Hatami and D. Jing, "Numerical analysis of nanofluids," in *Nanofluids: mathematical, numerical, and experimental analysis*, Cambridge, MA, USA: Academic Press, 2020, pp. 113–170.

[4] M. Hatami and D. Jing, "Nanofluid analysis in different applications," in *Nanofluids: mathematical, numerical, and experimental analysis*, Cambridge, MA, USA: Academic Press, 2020, pp. 283–347.

[5] S. Yasmin *et al.*, "Computational analysis of MHD MgO– water nanofluid flow inside hexagonal enclosure fitted with fins," *Case Studies in Thermal Engineering*, vol. 43, Mar. 2023, Art. no. 102788, https://doi.org/10.1016/j.csite.2023.102788.

[6] N. C. Roy, "MHD natural convection of a hybrid nanofluid in an enclosure with multiple heat sources," *Alexandria Engineering Journal*, vol. 61, no. 2, pp. 1679–1694, Feb. 2022, https://doi.org/10.1016/j.aej.2021.06.076.

[7] S. Nag, N. Sen, H. T. Bamboowala, N. K. Manna, N. Biswas, and D. K. Mandal, "MHD nanofluid heat transport in a corner-heated triangular enclosure at different inclinations," *Materials Today: Proceedings*, vol. 63, pp. 141–148, Jan. 2022, https://doi.org/10.1016/j.matpr.2022.02.421.

[8] M. Thangavelu, N. Nagarajan, and R.-J. Yang, "Magnetohydrodynamic Effect on Thermal Transport by Silver Nanofluid Flow in Enclosure with Central and Lower Heat Sources," *Heat Transfer Engineering*, vol. 43, no. 20, pp. 1755–1768, Sep. 2022, https://doi.org/10.1080/01457632.2021.2009226.

[9] F. Khan, Y. Xiao-Dong, N. Aamir, T. Saeed, and M. Ibrahim, "The effect of radiation on entropy and heat transfer of MHD nanofluids inside a quarter circular enclosure with a changing L-shaped source: lattice Boltzmann methods," *Chemical Engineering Communications*, vol. 210, no. 5, pp. 740–755, May 2023, https://doi.org/10.1080/00986445.2021.1990887.

[10] A. Yasmin, K. Ali, and M. Ashraf, "MHD Casson nanofluid flow in a square enclosure with non-uniform heating using the Brinkman model," *The European Physical Journal Plus*, vol. 136, no. 2, Jan. 2021, Art. no. 151, https://doi.org/10.1140/epjp/s13360-021-01093-9.

[11] T. Tayebi, H. F. Öztop, and A. J. Chamkha, "MHD natural convection of a CNT-based nanofluid-filled annular circular enclosure with inner heat-generating solid cylinder," *The European Physical Journal Plus*, vol. 136, no. 2, Jan. 2021, Art. no. 150, https://doi.org/10.1140/epjp/s13360-021-01106-7.

[12] H. Eshgarf, A. Ahmadi Nadooshan, A. Raisi, and M. Afrand, "Experimental examination of the properties of Fe3O4/water nanofluid, and an estimation of a correlation using an artificial neural network," *Journal of Molecular Liquids*, vol. 374, Mar. 2023, Art. no. 121150, https://doi.org/10.1016/j.molliq.2022.121150.

[13] M. F. Qasim, Z. K. Abbas, and S. K. Abed, "Producing Green Concrete with Plastic Waste and Nano Silica Sand," *Engineering, Technology & Applied Science Research*, vol. 11, no. 6, pp. 7932–7937, Dec. 2021, https://doi.org/10.48084/etasr.4593.

[14] S. Zeb, S. Gul, K. Shah, D. Santina, and N. Mlaiki, "Melting heat transfer and thermal radiation effects on MHD tangent hyperbolic nanofluid flow with chemical reaction and activation energy," *Thermal Science*, vol. 27, no. Spec. issue 1, pp. 253–261, 2023, https://doi.org/10.2298/TSCI23S1253Z.

[15] W. N. Muyungi, M. H. Mkwizu, and V. G. Masanja, "The Effect of Navier Slip and Skin Friction on Nanofluid Flow in a Porous Pipe," *Engineering, Technology & Applied Science Research*, vol. 12, no. 2, pp. 8342–8348, Apr. 2022, https://doi.org/10.48084/etasr.4763.

[16] H. A. Fakhim, "An Investigation of the Effect of Different Nanofluids in a Solar Collector," *Engineering, Technology & Applied Science Research*, vol. 7, no. 4, pp. 1741–1745, Aug. 2017, https://doi.org/10.48084/etasr.1283.

[17] R. Nciri, F. Alqurashi, C. Ali, and F. Nasri, "A Hydrodynamic–Elastic Numerical Case Study of a Solar Collector with a Double Enclosure Filled with Air and Fe3O4/Water Nanofluid," *Processes*, vol. 10, no. 6, Jun. 2022, Art. no. 1195, https://doi.org/10.3390/pr10061195.

[18] R. Nciri, Y. Ali Rothan, F. Nasri, and C. Ali, "Fe3O4-Water Nanofluid Free Convection within an Inclined 2D Rectangular Enclosure Heated by Solar Energy Using Finned Absorber Plate," *Applied Sciences*, vol. 11, no. 2, Jan. 2021, Art. no. 486, https://doi.org/10.3390/app11020486.

[19] F. Nasri, Y. Ali Rothan, R. Nciri, and C. Ali, "MHD Natural Convection of a Fe3O4–Water Nanofluid within an Inside Round Diagonal Corner Square Cavity with Existence of Magnetic Source," *Applied Sciences*, vol. 10, no. 9, Jan. 2020, Art. no. 3236, https://doi.org/10.3390/app10093236.